Polymer Brushes

Deutsche Ausgabe: DOI: 10.1002/ange.201607786
Internationale Ausgabe: DOI: 10.1002/anie.201607786

High-Density Liquid-Crystalline Polymer Brushes Formed by Surface Segregation and Self-Assembly

Koji Mukai, Mitsuo Hara, Shusaku Nagano, and Takahiro Seki**

Abstract: *High-density polymer brushes on substrates exhibit unique properties and functions stemming from the extended conformations due to the surface constraint. To date, such chain organizations have been mostly attained by synthetic strategies of surface-initiated living polymerization. We show herein a new method to prepare a high-density polymer brush architecture using surface segregation and self-assembly of diblock copolymers containing a side-chain liquid-crystalline polymer (SCLCP). The surface segregation is attained from a film of an amorphous base polymer (polystyrene, PS) containing a minor amount of a SCLCP-PS diblock copolymer upon annealing above the glass-transition temperature. The polystyrene portion of the diblock copolymer can work as a laterally mobile anchor for the favorable self-assembly on the polystyrene base film.*

The surface coatings of the polymer materials are of particular importance in industrial applications. Surface grafting of polymer chains is a promising method for surface modification. Grafting of polymer chains on substrate surfaces is primarily formed by chemical attachment achieved using the preformed polymer chains ("grafting-to"), surface-initiated (SI) polymerization ("grafting-from"),[1,2] and, more recently, polymerization using surface attached monomers ("grafting-through").[3] Among these, the "grafting-from" process using controlled living radical polymerizations has attracted particular attention because this method enables the preparation of highly dense polymer brushes with extended chain conformations oriented vertically from a substrate surface.[4–7] The thermal and mechanical properties of the high-density polymer brushes were significantly different compared with the unconstrained polymer chains in the spincast film.[8–11] Recently, various types of polymers have been applied and provide many useful surface functions, such as low friction,[10,12] wettability control,[13] and biocompatibility.[14]

SI living polymerization has also been harnessed to synthesize side-chain liquid-crystalline polymers (SCLCP).[15–18] The high-density brushes obtained using this procedure provide planarly oriented mesogens with an upright backbone orientation, which is in contrast with the cases of the homeotropic alignment observed for spincast films and Langmuir–Blodgett films of the corresponding polymers. This unique mesogen orientation is ascribed to the constraint effect on the surface with the attachment of one terminus of the chain. When a photoresponsive mesogen, such as azobenzene (Az), is used, the photoalignment of the mesogen is effectively achieved through the irradiation with linearly polarized light (LPL).[17,18]

On the other hand, the surface segregation of a selective polymer in blended amorphous polymer films has been extensively studied from the viewpoint of polymer physics and technological applications because it allows for low-cost, easy, and reliable surface modifications of polymer materials.[19–22] Low surface tension (hydrophobic) chains and higher entropic factors, such as low-molecular-weight substances, abundance in chain terminals, and highly flexible structures, promote segregation at the free surface.[22] The use of block copolymers as the segregating component provides even more interesting aspects. With block copolymers, various functional moieties can be readily introduced to the materials surface.[23–27] The lower free surface energy or a more flexible polymer block migrates to the free surface,[23–27] and an intermaterial dividing surface (IMDS) of the polymer blocks is formed parallel to the film plane with the main chain directing preferentially normal to the IMDS. Despite the accumulated data for the amorphous chain systems at the segregated state,[23–27] to the best of our knowledge, no attempts have been made to pursue the segregation process of SCLCP containing diblock copolymers on amorphous polymer films.

We show herein that high-density LC polymer brushes of SCLCP-*block*-polystyrene (PS) with planarly aligned mesogens are readily formed via surface segregation and self-assembly on a base PS film after appropriate thermal annealing as revealed by water contact angle measurements, X-ray photoelectron spectroscopy (XPS), transmission electron microscope (TEM), UV-visible absorption spectroscopy, and grazing angle incidence small-angle X-ray scattering (GI-SAXS). The key to the formation of ordered high-density polymer brushes is the allowed lateral mobility of the PS anchoring block above the glass transition temperature (T_g) of PS. This strategy is expected to offer a new versatile platform to prepare high-density polymer brushes without utilizing the synthetic procedure of SI living polymerization. We note that the surface segregation of photoresponsive SCLCP homopolymer or diblock copolymers containing an

[*] K. Mukai, Dr. M. Hara, Prof. T. Seki
Department of Molecular Design and Engineering
Graduate School of Engineering, Nagoya University
Furo-cho, Chikusa, Nagoya 464-8603 (Japan)
E-mail: tseki@apchem.nagoya-u.ac.jp
Prof. S. Nagano
Nagoya University Venture Business Laboratory
Furo-cho, Chikusa, Nagoya 464-8603 (Japan)
E-mail: snagano@apchem.nagoya-u.ac.jp
Supporting information and the ORCID identification number(s) for the author(s) of this article can be found under http://dx.doi.org/10.1002/anie.201607786.

azobenzene (Az) mesogen provides a new type of photoalignment system controlled from the free surface.[29–31]

Details of the syntheses and experimental procedures are described in the supporting information. Three liquid-crystalline (LC) diblock copolymers (PS-*b*-PAz, Scheme 1) were

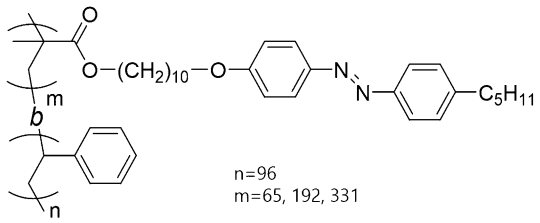

Scheme 1. Chemical structure of PS-*b*-PAz.

synthesized by activators regenerated by electron transfer atom transfer radical polymerization (ARGET ATRP) method[32] with a common PS macroinitiator ($M_n = 1.0 \times 10^4$, $M_w/M_n = 1.06$, average unit number (N) = 96). The molecular mass and the polydispersity of the three diblock copolymers (PS-*b*-PAz) were as follows: PS_{96}-*b*-PAz_{65} ($M_n = 4.2 \times 10^4$, $M_w/M_n = 1.29$), PS_{96}-*b*-PAz_{192} ($M_n = 1.05 \times 10^5$, $M_w/M_n = 1.38$), and PS_{96}-*b*-PAz_{331} ($M_n = 1.73 \times 10^5$, $M_w/M_n = 1.44$). The number-averaged molecular mass of the PS used for the base film and the Az homopolymer (PAz) were 1.94×10^5 ($M_w/M_n = 1.83$) and 8.8×10^4 ($M_w/M_n = 1.31$), respectively. The thermophysical properties evaluated using differential scanning calorimetry of the polymers were as follows: polystyrene: T_g = 105 °C; PAz: glass 58 °C, smectic C 82 °C, smectic A 114 °C, isotropic; PS-*b*-PAz: PAz: glass 56 °C, smectic C 90 °C, smectic A 114 °C, isotropic.[30]

Spincast films with a thickness of approximately 500 nm composed of binary mixtures of PS-*b*-PAz and PS (PS-*b*-PAz/PS film) were prepared from chloroform solutions. The mixing ratios of the PS-*b*-PAz and the PS were 5:95 (PS_{96}-*b*-PAz_{65}/PS film) or 10:90 (PS_{96}-*b*-PAz_{192}/PS and PS_{96}-*b*-PAz_{331}/PS films) by weight (see Figure S1 in the Supporting Information). In these conditions, an excessive amount of surface segregation or micelle formation of the diblock copolymer was avoided.[23] For pure polymer films, the thicknesses were 80 nm. All of the prepared films were annealed at 130 °C (higher than T_g of PS) for 24 h. The static contact angles of a water droplet (θ_w) on these films are summarized in Table 1. θ_w values for the pure PAz film exhibited a slight increase from 106° to 113° by annealing, which likely implies that there was exposure of the hydrophobic and mobile alkyl tail of the Az mesogen unit to the topmost surface. The pure PS film gave θ_w values of 95–96°, which was essentially unchanged by annealing. For the PS-*b*-PAz/PS mixture films after annealing, the θ_w values increased to a certain degree to 110–112°, and these values were significantly greater than that of pure PS film and close to that of pure PAz film. These results strongly suggest that the minor component of PS-*b*-PAz was segregated at the free surface of the PS film by annealing. The surface segregation of PS-*b*-PAz at the topmost film surface was further confirmed by X-ray photoelectron spectroscopy (XPS; Figures S2 and S3). The surface segregation of the PS-*b*-PAz should be driven by the lower surface energy and flexibility of the PAz block compared with PS.

Table 1: Contact angle of water (θ_w) on the polymer films.

Film	θ_w [deg]	
	As-cast state	After annealing
PAz	105.8 ± 0.9	113.4 ± 0.6
PS	94.6 ± 0.4	95.9 ± 1.0
PS_{96}-*b*-PA_{65} (5 wt%)/PS	107.2 ± 0.6	109.9 ± 0.4
PS_{96}-*b*-PAz_{192}(10 wt%)/PS	107.1 ± 0.1	110.7 ± 0.3
PS_{96}-*b*-PAz_{331}(10 wt%)/PS	107.9 ± 0.2	112.1 ± 0.5

For the TEM observation, the same blended polymer films were prepared on a Kapton (polyimide) substrate and were stained by exposure to a RuO_4 vapor. Figure 1 shows the cross-sectional TEM images of PS-*b*-PAz/PS films with varied PAz block length. In the images, a skin layer at the topmost surface (epoxy resin side) was clearly observed as a brighter band at the boundary. This surface skin layer can be assigned to the surface segregated PAz block for the following reasons. First, phenyl groups are more strongly stained with RuO_4.[33] The less-stained surface boundary layer should correspond to the PAz block with lower phenyl group density. Second, the thickness ratio of the skin layer to the entire film closely corresponds to the amount of added PAz components in the films. Third, θ_w and XPS data indicate that the topmost surface of the mixed film consists of the PAz component. As shown in Figure 1, the thickness of the segregated skin layer increased with the molecular weight (length) of the PAz block.

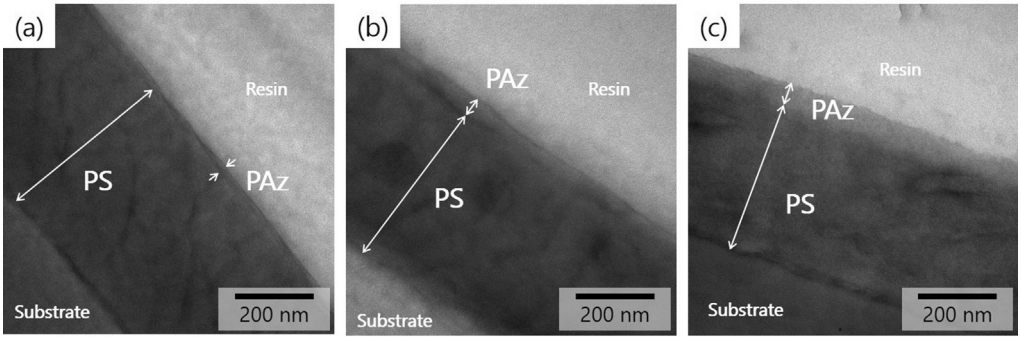

Figure 1. Cross-sectional TEM images of the PS_{96}-*b*-PAz_{65}(5 wt%)/PS film (a), the PS_{96}-*b*-PAz_{192}(10 wt%)/PS film (b), and the PS_{96}-*b*-PAz_{331}(10 wt%)/PS film (c). All polymer films were stained using RuO_4 vapor.

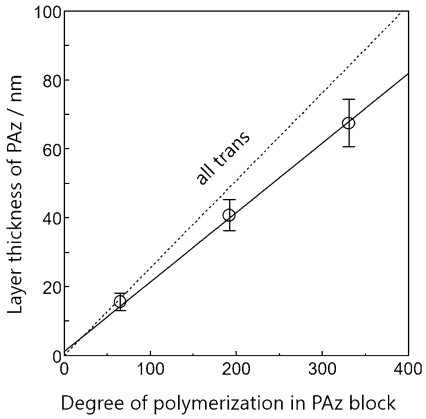

Figure 2. Relationship between the layer thickness of the surface-segregated PAz block and the degree of polymerization of the PAz block unit. The solid and dotted lines show the observed boundary layer thickness in the cross-sectional TEM (average of ten positions in Figure 3) and the ideally extended chain length in the all-*trans*-zigzag conformation, respectively.

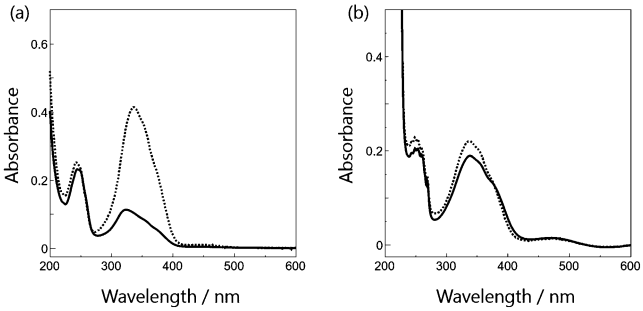

Figure 3. UV/Vis absorption spectra of the PS_{96}-*b*-PAz_{192} film (a) and PS_{96}-*b*-PAz_{192}(10 wt%)/PS film (b). The dotted and solid lines indicate spectra of the as-cast and the annealed films, respectively.

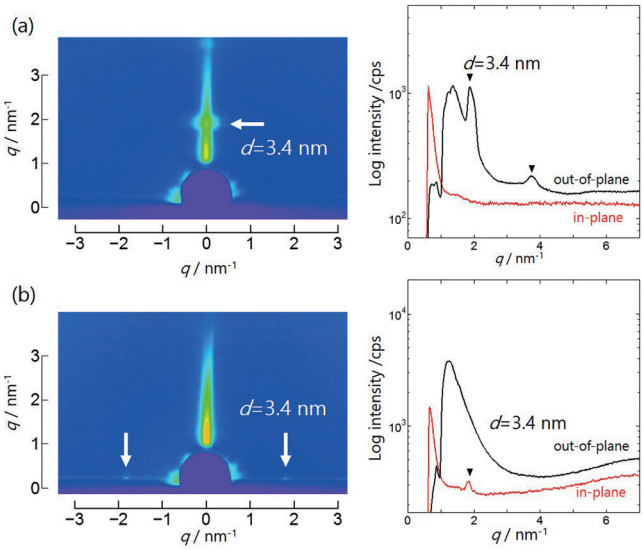

Figure 4. GI-SAXS 2D pattern image of the pure PS_{96}-*b*-PAz_{192} film at 95 °C (a) and the PS_{96}-*b*-PAz_{192}/PS film at 95 °C (b). Corresponding GI-SAXS 1D intensity profiles are shown on the right side.

Figure 2 shows the thickness of the observed PAz skin layer plotted against the degree of polymerization (N) of the PAz block chain. The thickness of the observed PAz layers proportionally increased with N of the PAz block chain. The slope of the approximated line between the skin layer thickness and the N of PAz block chain was $0.202N$ [nm]. The calculated poly(methyl methacrylate) (PMMA) length of the all-*trans*-zigzag conformation is given by $0.254N$ [nm][10] (dotted line in Figure 2). Therefore, the length of the PAz block chains reaches approximately 80% of the all-*trans*-zigzag conformation of PMMA, which indicates that the surface segregated PAz chains adopt highly extended conformations (polymer brush structure) in the skin layer. For high-density amorphous brushes, such as PMMA, the thickness in the dry state is known to reach 40% of the fully extended chain length.[6] In the present case, the magnitude of extension (80%) is worth mentioning, which should stem from the existence of the self-assembling bulky mesogens at each repeating unit. We assume that such high main-chain extension is caused by the smectic layer formation. A nematic state that allows a more mobility freedom of mesogens does not seem to provide extended chain conformations.

To gain further insight into the structure of the PAz block brush, the UV/Vis absorption spectra of pure PS_{96}-*b*-PAz_{192} and mixed PS_{96}-*b*-PAz_{192}/PS films were taken on a fused silica substrate (Figure 3). The absorption peak of the π-π* transition band of the Az moiety was observed at 337 nm in the as-cast state for both films. After annealing, conversely, the π-π* bands exhibit quite different relationship between the pure PS-*b*-PAz and PS-*b*-PAz/PS films. In the pure film, the absorbance of the π-π* transition band was largely reduced (27% of the as-cast film), and the maximum absorption wavelength (λ_{max}) showed a blue-shift from 337 nm to 323 nm. The reduction of the intensity and peak shift indicate that the mesogens of PS-*b*-PAz were aligned homeotropically with the H-aggregation.[16–18] In the PS-*b*-PAz/PS film, in contrast, the absorbance and λ_{max} of the π-π* transition band was almost unchanged. Therefore, the mesogens in the annealed PS_{96}-*b*-PAz_{192} adopts random or planar orientations. The same tendency was observed in the PS_{96}-*b*-PAz_{65}/PS and PS_{96}-*b*-PAz_{331}/PS films (Figure S4).

Figure 4 shows the 2D GI-SAXS images of pure PS_{96}-*b*-PAz_{192} and PS_{96}-*b*-PAz_{192}/PS films measured at a smectic A phase temperature (95 °C). The scattering from the pure PS_{96}-*b*-PAz_{192} film was detected only in the out-of-plane direction with scattering vector (q) values being 1.87 nm^{-1} (the layer spacing, $d = 3.4$ nm) and 3.77 nm^{-1} ($d = 1.7$ nm) (Figure 4a). These scatterings were attributed to the first- and second-order scatterings from the smectic lamella oriented horizontally to the surface.[16–18,29] Conversely, in the mixed PS-*b*-PAz/PS film, X-ray scatterings were observed only in the in-plane direction at $q = 1.83$ nm^{-1} ($d = 3.4$ nm). The in-plane scattering indicates that the smectic lamellar of PAz was formed vertically to the surface. Essentially, the same data were obtained for the other polymers of PS_{96}-*b*-PAz_{65} and PS_{96}-*b*-PAz_{331} (Figures S5 and S6).

Generally, thin films of SCLCP tend to adopt a homeotropic alignment, which is explained in terms of the excluded volume theory of the side chain at the free interface.[34] Actually, the PAz homopolymer and LC azobenzene diblock copolymers with a poly(ethylene oxide)[35] and PS[36] block exhibit a homeotropic orientation in a thin film state (Figure 5a). Mesogen orientations over the whole thickness of thin films are dominated by the orientation at the free surface.[37] In this state, the PS cylinders are also oriented vertically.[35,36] As demonstrated in this work, the surface segregated PAz block shows a unique random planar orientation at the free surface (Figure 5b). By mixing a moderate amount of the PS-*b*-PAz additive in the base PS films, the segregated PAz block formed a quasi-monolayer with the miscible PS chains anchored to the base PS film. This brush forming process should be promoted by two factors. i) The lower surface tension of the PAz blocks and miscibility of the PS block with the base PS can induce surface segregation with an IMDS on the PS film surface.[38] ii) The self-assembling LC nature of the PAz block facilitates the dense packing to form a smectic A structure, which is similar to a zipper arrangement. Through such thermodynamic requirements, the main chains of the PAz block should be highly stretched perpendicular to the surface. The difference in the SCLCP length may change the kinetics of the brush formation. However, the kinetics seems to be similar in the procedures adopted because the annealing is commonly achieved above the isotropization temperature of PAz.

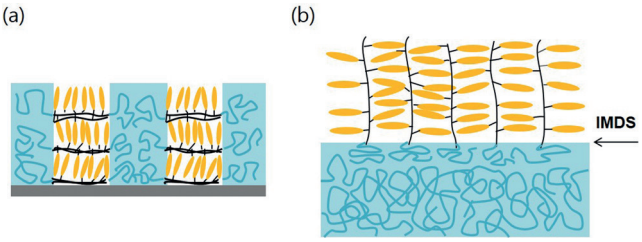

Figure 5. Schematic depictions of the mesogen orientation of PS-*b*-PAz in the pure PS-*b*-PAz film (a) and the PS-*b*-PAz/PS film (b) after annealing.

Formation of the LC polymer brush structure can be compared with that of widely studied self-assembled monolayers (SAMs) of alkanthiols on Au surfaces.[39] The high ordering of such SAMs is based on the lateral van der Waals attractive interaction between molecules and allowed lateral mobility with moderate interactions with the surface. We assume that the ordering of the PAz block in the present case progresses in the same manner. The lateral interaction between the PAz blocks is favored by the aggregation of mesogens, and additionally, the lateral mobility of the PS block anchor is allowed at temperatures higher than T_g. In this way, one can find such similarities in both processes. The present system can be regarded as a SAM of macromolecules at a mesoscopic scale.

Rough estimations can be made for the dimension of a single-block copolymer chain of PS-*b*-PAz in the segregated state (supporting information). Assuming the densities of PAz to be 1.0 g cm^{-3}, a single block of the PS_{96}-*b*-PAz_{192} chain ($M_n = 9.0 \times 10^4$), for example, should occupy a volume of 150 nm^3. The PAz block with 3.4-nm layer spacing (see Figure 4b) and 40-nm chain extension (see Figure 2) gives 1 nm width per chain. Because the molecular weight of the anchor PS block (1.0×10^4) is much less than that of the base PS film (1.9×10^5), the penetration of mutual PS chain would not effectively occur.[38] If this is the case, the depth of the PS anchor block should range a several nanometer level form the IMDS.

As shown earlier, the similar random planar orientation of PAz is obtained in the PAz polymer brush prepared by the SI living polymerization on the solid surfaces.[16–18] The new approach proposed here has significant advantages as follows. First, the procedure is very simple without requiring a skillful procedure as in SI living polymerization. The thickness of the brush is precisely adjusted using well-characterized preformed diblock copolymers. Second, the polymer brush surfaces can be prepared on flexible polymer substrates. This will provide wider opportunities for materials processing. Third, we anticipate that, even if a part of the surface brush layer is damaged, it will be recovered by annealing as far as the buried block copolymer components still remain (antifouling effect). Yokoyama et al.[25,26] demonstrated that amphiphilic diblock copolymers containing poly(ethylene oxide) block or oligo(ethylene oxide) side chain polymer block spontaneously form high-density polymer brushes through surface segregation in contact with water. Such brush structure is reconstituted when the water phase is removed. In our system, conversely, the surface segregated brush structure is formed and retained stably in the air. These facts indicate that the both approaches are complimentary from the viewpoint of surface processing of polymer materials.

Finally, the segregated PAz brush on the PS film was subjected the photoalignment by irradiation with LPL at 436 nm. Preliminary experiments indicated that the Az mesogens were aligned orthogonal to the electric vector of LPL with an orientational order parameter estimated using optical anisotropy[16–18] of 0.54 at 90 °C (Figure S8). This value is comparable with those obtained for high-density PAz brushes prepared using SI living polymerization.[16–18] Therefore, the surface segregated PAz brush behaves in a similar manner as the high-density brushes obtained using grafting-from synthesis. The details of the photoalignment behavior will be reported in due course.

In summary, a simple strategy to prepare high-density polymer brushes of SCLCP using surface segregation is proposed. A small amount of PS-*b*-PAz blended in a PS base film is segregated to the free surface by annealing at a temperature higher than T_g of PS. The high-density brush formation can be ascribed to the lateral self-assembly of SCLCP and the allowed mobility of the PS anchor. The thickness of the segregated PAz block reaches 80% of the fully extended all-*trans*-zigzag conformation state. The resulting structure and photoalignment ability are highly analogous to that obtained by the brushes using SI living polymerization; however, the present approach offers more precise and reproducible brush architectures through the use of pre-

formed diblock copolymers that have a defined structure and molecular weight. We are also currently making efforts to extend this strategy to other types of LC polymer systems

Acknowledgements

This work was supported by Japan Society for the Promotion of Science grant numbers JP15H01084, JP16H06355, and JP15K13784.

Keywords: azo compounds · liquid crystals · polymers · self-assembly · thin films

How to cite: *Angew. Chem. Int. Ed.* **2016**, *55*, 14028–14032
Angew. Chem. **2016**, *128*, 14234–14238

[1] R. C. Advincula, W. J. Brittain, K. C. Caster, J. Rühe, *Polymer Brushes*, Wiley-VCH, Weinheim, **2004**.
[2] "Surface-Initiated Polymerization": R. Jordan, *Advances in Polymer Science*, *Vol. 197* and *198*, Springer, Berlin, **2006**.
[3] M. Henze, D. Mädge, O. Prucker, J. Rühe, *Macromolecules* **2014**, *47*, 2929–2938.
[4] S. Edmondson, V. L. Osborne, W. T. S. Huck, *Chem. Soc. Rev.* **2004**, *33*, 14–22.
[5] S. Minko, *Polym. Rev.* **2006**, *46*, 397–420.
[6] Y. Tsujii, K. Ohno, S. Yamamoto, A. Goto, T. Fukuda, *Adv. Polym. Sci.* **2006**, *197*, 1–45.
[7] A. Kopyshev, C. J. Galvin, J. Genzer, N. Lomadze, S. Santer, *Langmuir* **2013**, *29*, 13967–13974.
[8] S. Yamamoto, M. Ejaz, Y. Tsujii, T. Fukuda, *Macromolecules* **2000**, *33*, 5608–5612.
[9] S. Yamamoto, Y. Tsujii, T. Fukuda, *Macromolecules* **2002**, *35*, 6077–6079.
[10] A. Nomura, K. Okayasu, K. Ohno, T. Fukuda, Y. Tsujii, *Macromolecules* **2011**, *44*, 5013–5019.
[11] K. Tanaka, K. Kojio, R. Kimura, A. Takahara, T. Kajiyama, *Polym. J.* **2003**, *35*, 44–49.
[12] M. Kobayashi, Y. Terayama, N. Hosaka, M. Kaido, A. Suzuki, N. Yamada, N. Torikai, K. Ishihara, A. Takahara, *Soft Matter* **2007**, *3*, 740–746.
[13] M. Kobayashi, Y. Terayama, H. Yamaguchi, M. Terada, D. Murakami, K. Ishihara, A. Takahara, *Langmuir* **2012**, *28*, 7212–7222.
[14] W. Feng, S. Zhu, K. Ishihara, J. L. Brash, *Langmuir* **2005**, *21*, 5980–5987.
[15] P. J. Hamelinck, W. T. S. Huck, *J. Mater. Chem.* **2005**, *15*, 381–385.
[16] T. Uekusa, S. Nagano, T. Seki, *Langmuir* **2007**, *23*, 4642–4645.
[17] T. Uekusa, S. Nagano, T. Seki, *Macromolecules* **2009**, *42*, 312–318.
[18] H. A. Haque, S. Kakehi, M. Hara, S. Nagano, T. Seki, *Langmuir* **2013**, *29*, 7571–7575.
[19] Q. S. Bhatia, D. H. Pan, J. T. Koberstein, *Macromolecules* **1988**, *21*, 2166–2175.
[20] R. A. L. Jones, E. J. Kramer, *Polymer* **1993**, *34*, 115–118.
[21] T. F. Schaub, G. J. Kellogg, A. M. Mayes, R. Kulasekere, J. F. Ankner, H. Kaiser, *Macromolecules* **1996**, *29*, 3982–3990.
[22] D. Kawaguchi, K. Tanaka, N. Torikai, A. Takahara, T. Kajiyama, *Langmuir* **2007**, *23*, 7269–7275.
[23] D. R. Iyengar, S. M. Perutz, C. A. Dai, C. K. Ober, E. J. Kramer, *Macromolecules* **1996**, *29*, 1229–1234.
[24] H. Lee, L. A. Archer, *Macromolecules* **2001**, *34*, 4572–4579.
[25] H. Yokoyama, T. Miyamae, S. Han, T. Ishizon, K. Tanaka, A. Takahara, N. Torikai, *Macromolecules* **2005**, *38*, 5180–5189.
[26] M. Inutsuka, N. L. Yamada, K. Ito, H. Yokoyama, *ACS Macro Lett.* **2013**, *2*, 265–268.
[27] A. Bousquet, E. Ibarboure, C. Drummond, C. Labrugère, E. Papon, J. Rodriguez-Hernandez, *Macromolecules* **2008**, *41*, 1053–1056.
[28] C. Zhang, Y. Oda, D. Kawaguchi, S. Kanaoka, S. Aoshima, K. Tanaka, *Chem. Lett.* **2015**, *44*, 166–168.
[29] K. Fukuhara, Y. Fujii, Y. Nagashima, M. Hara, S. Nagano, T. Seki, *Angew. Chem. Int. Ed.* **2013**, *52*, 5988–5991; *Angew. Chem.* **2013**, *125*, 6104–6107.
[30] K. Fukuhara, S. Nagano, M. Hara, T. Seki, *Nat. Commun.* **2014**, *5*, 3321–3328.
[31] T. Nakai, D. Tanaka, M. Hara, S. Nagano, T. Seki, *Langmuir* **2016**, *32*, 909–914.
[32] W. Jakubowski, K. Min, K. Matyjaszewski, *Macromolecules* **2006**, *39*, 39–45.
[33] U. A. Spitzer, D. G. Lee, *J. Org. Chem.* **1974**, *39*, 2468–2469.
[34] H. Kimura, H. Nakano, *J. Phys. Soc. Jpn.* **1985**, *54*, 1730–1736.
[35] S. Asaoka, T. Uekusa, H. Tokimori, M. Komura, T. Iyoda, T. Yamada, H. Yoshida, *Macromolecules* **2011**, *44*, 7645–7658.
[36] Y. Morikawa, T. Kondo, S. Nagano, T. Seki, *Chem. Mater.* **2007**, *19*, 1540–1542.
[37] D. Tanaka, Y. Nagashima, M. Hara, S. Nagano, T. Seki, *Langmuir* **2015**, *31*, 11379–11383.
[38] K. H. Dai, E. J. Kramer, K. R. Shull, *Macromolecules* **1992**, *25*, 220–225.
[39] J. C. Love, L. A. Estroff, J. K. Kriebel, R. G. Nuzzo, G. M. Whitesides, *Chem. Rev.* **2005**, *105*, 1103–1170.

Received: August 10, 2016
Revised: September 13, 2016
Published online: October 11, 2016

